Marriage between neutrino mass and flavor anomalies

J. Julio,[1,*] Shaikh Saad,[2,†] and Anil Thapa[3,‡]

[1]*National Research and Innovation Agency, Kompleks Puspiptek Serpong, South Tangerang 15314, Indonesia*

[2]*Department of Physics, University of Basel, Klingelbergstrasse 82, CH-4056 Basel, Switzerland*

[3]*Department of Physics, University of Virginia, Charlottesville, Virginia 22904-4714, USA*

(Received 8 April 2022; accepted 16 August 2022; published 6 September 2022)

Experimental hints for lepton flavor universality violation in beauty-quark decay both in neutral- and charged-current transitions require an extension of the Standard Model for which scalar leptoquarks (LQs) are the prime candidates. Besides, these same LQs can resolve the long-standing tension in the muon and the recently reported deviation in the electron $g-2$ anomalies. These tantalizing flavor anomalies have discrepancies in the range of $2.5\sigma - 4.2\sigma$, indicating that the Standard Model of particle physics may finally be cracking. In this Article, we propose a resolution to all these anomalies within a unified framework that sheds light on the origin of neutrino mass. In this model, the LQs that address flavor anomalies run through the loops and generate neutrino mass at the two-loop order while satisfying all constraints from collider searches, including those from flavor physics.

DOI: 10.1103/PhysRevD.106.055003

I. INTRODUCTION

In the Standard Model (SM), the coupling of the electroweak (EW) gauge bosons to leptons is flavor universal, a property known as lepton flavor universality (LFU). The SM's extension is expected to violate this property, and experimental observations of such processes will be direct evidence of physics beyond the SM (BSM). Even though LHC searches have not found any direct hints for new particles, indirect searches for new physics have become an increasingly important pathway. Intriguing hints for BSM physics have accumulated over the years from the measurements of precision observables in several experiments that strongly suggest LFU violation (LFUV).

Lepton anomalous magnetic moments (AMMs) for the first two generations that are very sensitive to new physics are measured in the experiments with unprecedented accuracy. There is a long-standing tension in the muon AMM $(g-2)_\mu$ measured in 2006 at Brookhaven [1]. Fermilab's new measurement [2] is in complete agreement with the previous result, and the combined result shows a large $+4.2\sigma$ discrepancy with the SM prediction [3]. For a recent review of BSM models addressing this anomaly, see Ref. [4]. As for the electron, a recent experiment at Berkeley [5] has measured the fine-structure constant using cesium atom with extreme precision, which indicates a -2.4σ disagreement with the direct experimental measurement [6]. A large positive deviation of $(g-2)_\mu$ but a negative deviation of $(g-2)_e$ has caused excitement in the high-energy physics community, and various new physics proposals have been made to solve these discrepancies simultaneously [7–58].

Here we point out that a more recent measurement utilizing rubidium atom at the Kastler Brossel Laboratory in Paris [59] is somewhat consistent with the direct experimental measurement [6]. Contrary to the 2018 result by Berkeley National Laboratory [5], this new 2020 result [59] finds Δa_e to be positive ($+1.6\sigma$), indicating a $\sim 5\sigma$ disagreement between these two experiments. Since these determinations by the two groups cannot be reconciled within the stated uncertainties, we, at first, will treat these two results as independent cases, presenting separate fits to demonstrate consistency of our model with each result. Later, however, we also perform a fit to illustrate how our model can be simultaneously consistent with the combined results of [5,59], favoring a Standard Model-like value.

Furthermore, LFU violating B-meson decays have been persistently observed in a series of experiments. Among these processes, the most prominent deviation has been observed in neutral-current transitions associated with the ratio: $R_{K^{(*)}} = \mathrm{Br}(B \to K^{(*)}\mu^+\mu^-)/Br(B \to K^{(*)}e^+e^-)$, which has very small theory uncertainties since hadronic uncertainties cancel out in the above ratios, making it extremely sensitive to new physics probes. In the SM, this

*julio@brin.go.id
†shaikh.saad@unibas.ch
‡wtd8kz@virginia.edu

ratio is predicted to be unity [60–64] due to the LFU property. However, experiments have consistently found it to be somewhat smaller than one [65–68]; among them, the most precise measurement by LHCb [69] alone quotes a significance of 3.1σ for R_K-ratio.[1] On the other hand, charged-current transitions in the B-meson decays indicate an enhancement of the ratio: $R_{D^{(*)}} = Br(B \to D^{(*)}\tau\bar{\nu}_\tau)/Br(B \to D^{(*)}\ell\bar{\nu})$, with $\ell = e, \mu$. The ratios $R_{D^{(*)}}$ show deviations [82–86] from the SM predictions [87,88] with a combined significance of about 3σ [89].

Besides all this, first and foremost, it is widely accepted that the SM cannot be the fundamental theory at all energies since it fails to incorporate neutrino oscillations firmly confirmed by various experiments; for reviews see Refs. [90,91]. Motivated by this crucial drawback of the SM, in this Article, we propose a simultaneous solution to all four of the anomalies mentioned above that are directly intertwined with the neutrino mass generation mechanism. In this unified framework [92], we employ two scalar leptoquarks[2] (LQs), $\{S_1(\bar{3}, 1, 1/3), R_2(3, 2, 7/6)\}$, which address the flavor anomalies and neutrino masses simultaneously. In this model, Majorana neutrino mass appears at two-loop order. Our novel proposal is minimal, and the *only neutrino mass model* in the literature that resolves all of these aforementioned notable anomalies while satisfying low-energy flavor constraints and the LHC limits.[3] Furthermore, the proposed model is fully testable since a resolution of the charged-current B-anomaly requires the relevant LQ to have a mass around 1 TeV (the neutral-current and $g-2$ anomalies can be explained with relatively heavier LQ).

This paper is organized in the following way: we introduce the model in Sec. II and discuss how anomalies are incorporated within this setup in Secs. III and IV. After presenting our numerical results in Sec. V, finally we conclude in Sec. VI.

II. MODEL

In addition to the SM particle content, the proposed model consists of two scalar LQs (SLQs), $S_1(\bar{3}, 1, +1/3)$, $R_2(3, 2, 7/6)$, and another BSM multiplet $\xi_3(3, 3, 2/3)$. We denote their component fields by

$$R_2 = \begin{pmatrix} R^{5/3} \\ R^{2/3} \end{pmatrix}, \quad S_1 = S^{1/3}, \quad \xi = \begin{pmatrix} \frac{\xi^{2/3}}{\sqrt{2}} & \xi^{5/3} \\ \xi^{-1/3} & -\frac{\xi^{2/3}}{\sqrt{2}} \end{pmatrix}.$$

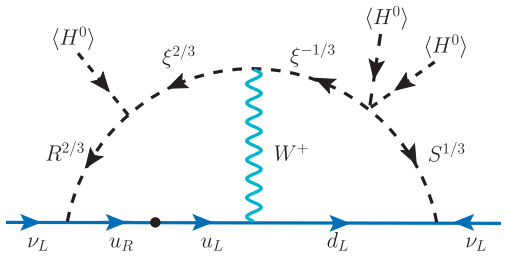

FIG. 1. A typical two-loop diagram leading to nonzero neutrino mass. For a full set of diagrams, see Ref. [92].

The couplings of LQs with the SM fermions take the following form:

$$\mathcal{L}_Y^{\text{new}} = f_{ij}^L \bar{u}_{Ri} R_2 \cdot L_j + f_{ij}^R \overline{Q}_i R_2 \ell_{Rj} + y_{ij}^L \overline{Q_i^c} \cdot L_j S_1 + y_{ij}^R \overline{u^c}_{Ri} S_1 \ell_{Rj}, \tag{1}$$

where Q and L stand for, respectively, left-handed quark and lepton doublets, u_R and ℓ_R are right-handed up-type quark and lepton, and $i, j = 1$–3 are family indices. We also use "$\cdot$" to denote $SU(2)$ contraction so that $L \cdot Q \equiv L^\rho Q^\sigma \epsilon_{\rho\sigma}$ with ϵ being the Levi-Civita tensor and $\rho, \sigma =$ being $SU(2)$ indices. Since explanations of flavor anomalies require that these LQs couple to quark-lepton bilinears, as usual, we turn off the diquark coupling of S_1 LQ, which guarantees baryon number conservation. Now, expanding these Yukawa terms, we obtain

$$\begin{aligned}\mathcal{L} = {} & \bar{u}_{Ri}(f^L)_{ij}\ell_{Lj}R^{5/3} + \bar{u}_{Ri}(-f^L)_{ij}\nu_{Lj}R^{2/3} \\ & + \bar{u}_{Li}(f^R)_{ij}\ell_{Rj}R^{5/3} + \bar{d}_{Li}(V^\dagger f^R)_{ij}\ell_{Rj}R^{2/3} \\ & + \overline{u^c}_{Li}(y^L)_{ij}\ell_{Lj}S^{1/3} + \overline{d^c}_{Li}(-V^T y^L)_{ij}\nu_{Lj}S^{1/3} \\ & + \overline{u^c}_{Ri}(y^R)_{ij}\ell_{Rj}S^{1/3},\end{aligned} \tag{2}$$

where, V represents the CKM mixing matrix, and we have chosen to work in the so-called "up-quark mass diagonal basis".

The two LQs and ξ can also interact with Higgs doublet H in the scalar potential $V_{sc} \supset \lambda S_1^\dagger H^T \epsilon \xi^\dagger H + \mu R_2^\dagger \xi H$. The simultaneous presence of the Yukawa and these scalar interactions breaks the lepton number by two units, as required for generating nonzero neutrino mass; one of the diagrams is shown in Fig. 1. If the Yukawa interactions are turned off, the leptoquarks are not required to carry any lepton number; hence the scalar potential will remain

[1] In addition to the clean observable $R_{K^{(*)}}$, several other observables are in tension with the SM predictions for example angular distributions and branching ratios of several $b \to s\mu^+\mu^-$ modes [70–79]. When all these anomalies are combined, a global fit [80,81] to data suggests $>5\sigma$ discrepancy. In this Article, we only focus on the $R_{K^{(*)}}$ ratio; the rest of the observables suffer from large hadronic uncertainties, and we do not attempt to alleviate these discrepancies.

[2] For a recent review on LQs, see Ref. [93]. Moreover, for solutions to B-anomalies by employing leptoquarks (scalar and vector) see e.g., Refs. [92,94–197].

[3] A few proposals of neutrino mass models attempted to connect neutrino mass with flavor anomalies; however, these models address these anomalies only partially; for details, see Ref. [92].

lepton-number conserving. After the EW symmetry breaking, these terms induce mixing in the LQ-ξ sector, yielding six physical exotic scalars, i.e., $\chi_a^{1/3}$, $\chi_a^{2/3}$, and $\chi_a^{5/3}$ with $a = 1, 2$. Since explaining flavor anomalies requires some $\mathcal{O}(1)$ Yukawa couplings, we are compelled, by tiny neutrino masses, to have small mixing angles. Therefore, it is a good approximation to identify gauge eigenstates $R^{2/3,5/3}$ and $S^{1/3}$ as their physical eigenstates.

In the chosen basis, the neutrino mass formula takes the following form:

$$\mathcal{M}_\nu = m_0 I_0 \Big\{ 2(y^L)^T D_u f^L + \frac{m_\tau}{m_t} D_\ell (y^R)^T f^L - \frac{m_\tau}{m_t} D_\ell (f^R)^T y^L \Big\} + \text{transpose}, \quad (3)$$

where $m_0 = 3g^2 m_t/\sqrt{2}(16\pi^2)^2$ with g being the $SU(2)$ gauge coupling constant and m_t being the top-quark mass. The normalized mass matrices of up-type quarks and charged leptons are $D_u = \text{diag}(\frac{m_u}{m_t}, \frac{m_c}{m_t}, 1)$ and $D_\ell = \text{diag}(\frac{m_e}{m_\tau}, \frac{m_\mu}{m_\tau}, 1)$. The loop integral I_0 in the asymptotic limit (i.e., when all fermion masses are zero) is given by

$$I_0 = \frac{1}{4} \sin 2\theta \sin 2\phi \sum_{a,b=1}^{2} (-1)^{a+b} I(M_{a+2}, M_b). \quad (4)$$

Here θ and ϕ denote the mixing angles of LQ with charges $1/3$ and $2/3$, respectively, while

$$I(M_{a+2}, M_b) = 8\left(1 - \frac{3}{4}\frac{M_{a+2}}{M_b}\right) - \frac{5}{6}\pi^2\left(1 - \frac{2}{5}\frac{M_{a+2}}{M_b}\right) + \frac{M_b^2}{m_W^2}\left(\frac{M_{a+2}}{M_b} - 1\right)\left(2 - \frac{1}{3}\pi^2\right) + \left(\frac{2M_{a+2}}{M_b} - 1\right)\ln\frac{m_W^2}{M_b^2} \quad (5)$$

is the loop function, derived by assuming $M_b/M_{a+2} = 1 + r_{ba}$ with $r_{ba} \ll 1$. Note that $M_{1,2}$ are masses for $2/3$ charged LQs and $M_{3,4}$ are for $1/3$ charged LQ. For more detailed discussion, we refer the reader to Ref. [92].

III. CORRELATED OBSERVABLES

This section discusses the relevant correlated observables/constraints in the proposed two-loop neutrino mass model that resolve the four anomalies.

At tree-level both S_1 and R_2 LQs contribute to the $b \to c\tau\bar{\nu}$ transition which are favorable, whereas they do not lead to a desired contribution to the $b \to s\mu\mu$. Loop-induced contributions to $b \to s\mu\mu$ transition face several difficulties and unable to consistently solve $R_{K^{(*)}}$ anomalies (see e.g., Ref. [174]). On the contrary, if R_2 LQ couples to the electrons, relatively small couplings are feasible to address [154,198] $R_{K^{(*)}}$ anomalies since the relevant operator is generated at the tree-level. Moreover, each of these LQs can also simultaneously explain both the $(g-2)_\mu$ and $(g-2)_e$ anomalies via the chirally enhanced top-quark and charm-quark contributions, respectively [33].

TABLE I. Constraints on Yukawa couplings from radiative decay of charged leptons. Here $\mathcal{C} = (1 + 4\log\frac{m_q^2}{M_{R_2}^2})$. The second (first) row in the "Constraints" column shows the bound with (without) chiral enhancement. Constraints on the S_1 LQ couplings $y^{L,R}$ with no chiral enhancement is weaker by a factor of 3, whereas chirally enhanced contribution has the factor with C replaced by $C' = (7 + 4\log\frac{m_q^2}{M_{R_2}^2})$. The contribution from $\hat{f}^R$ is suppressed as it is proportional to $m_b^2/M_{R_2}^2$ in comparison to $R_2^{5/3}$.

Process	Constraints
$\mu \to e\gamma$ [200]	$\lvert f^R_{ae} f^{R*}_{a\mu}\rvert + \lvert f^L_{ae} f^{L*}_{a\mu}\rvert < 4.82 \times 10^{-4}\ (\frac{M_{R_2}}{\text{TeV}})^2$
	$(\lvert f^R_{ae} f^{L*}_{a\mu}\rvert + \lvert f^L_{ae} f^{R*}_{a\mu}\rvert)\mathcal{C} < 7.63 \times 10^{-5}$
	$(\frac{M_{R_2}}{\text{TeV}})^2\ (\frac{1\ \text{GeV}}{m_q})$
$\tau \to e\gamma$ [201]	$\lvert f^R_{ae} f^{R*}_{a\tau}\rvert + \lvert f^L_{ae} f^{L*}_{a\tau}\rvert < 0.32\ (\frac{M_{R_2}}{\text{TeV}})^2$
	$(\lvert f^R_{ae} f^{L*}_{a\tau}\rvert + \lvert f^L_{ae} f^{R*}_{a\tau}\rvert)\mathcal{C} < 0.85\ (\frac{M_{R_2}}{\text{TeV}})^2\ (\frac{1\ \text{GeV}}{m_q})$
$\tau \to \mu\gamma$ [201]	$\lvert f^R_{a\mu} f^{R*}_{a\tau}\rvert + \lvert f^L_{a\mu} f^{L*}_{a\tau}\rvert < 0.37\ (\frac{M_{R_2}}{\text{TeV}})^2$
	$(\lvert f^R_{a\mu} f^{L*}_{a\tau}\rvert + \lvert f^L_{a\mu} f^{R*}_{a\tau}\rvert)\mathcal{C} < 0.98\ (\frac{M_{R_2}}{\text{TeV}})^2\ (\frac{1\ \text{GeV}}{m_q})$
$\mu - e$ [202]	$\lvert \hat{f}^R_{ue} \hat{f}^{R*}_{u\mu}\rvert \le 8.58 \times 10^{-6}\ (\frac{M_{R_2}}{\text{TeV}})^2$

To be specific, $\hat{f}^R_{se,be}$ (for brevity, we define $\hat{f}^R \equiv V^\dagger f^R$ and $\hat{y}^L \equiv -V^T y^L$) couplings are responsible for addressing $R_{K^{(*)}}$ anomalies. Incorporating the $(g-2)_\mu$ ($(g-2)_e$) anomaly requires either $f^{R,L}_{t\mu}$ or $y^{R,L}_{t\mu}$ ($f^{R,L}_{t/ce}$ or $y^{R,L}_{t/ce}$) couplings to be sizable. Furthermore, with TeV scale LQ (LQ mass below TeV is highly constrained by LHC data), explanations of $R_{D^{(*)}}$ anomalies typically demand $\mathcal{O}(1)$ $y^R_{c\tau}$ and $\hat{y}^L_{b\ell}$ ($\hat{f}^R_{b\tau}$ and $f^L_{c\ell}$) entries if S_1 (R_2) LQ is responsible for this charged-current processes.

Consequently, the NP contribution to resolving these four anomalies while incorporating neutrino oscillation data is highly nontrivial and leads the way to various flavor violating processes that are severely constrained by the experimental data. One of the most important constraints is the lepton flavor violating (LVF) radiative decay of charged leptons $\ell_i \to \ell_j\gamma$ [199]. For instance, the $\mu \to e\gamma$ process precludes R_2 LQ to accommodate Δa_μ while resolving $R_{K^{(*)}}$. Furthermore, to avoid strong constraints from chirally enhanced $\ell_i \to \ell_j\gamma$ via the CKM rotation in the up-sector, we have chosen to work in the up-quark mass diagonal basis of Eq. (2). Constraints on the Yukawa couplings owing to dominant LVF processes as a function of LQ mass for both nonchiral and chirally enhanced diagrams are shown in Table I together with constraint from coherent $\mu - e$ conversion in nuclei.

TABLE II. Constraints on the relevant LQ couplings as a function of mass from leptonic kaon and B meson decays.

Process	Constraints [203–205]
$K_L \to e^+e^-$	$\lvert\hat{f}^R_{de}\hat{f}^{R*}_{se}\rvert \le 2.0\times10^{-3}\ (\frac{M_{R_2}}{\text{TeV}})^2$
$K^0_L \to e^\pm\mu^\mp$	$\lvert\hat{f}^R_{d\mu}\hat{f}^{R*}_{se}+\hat{f}^R_{s\mu}\hat{f}^{R*}_{de}\rvert \le 1.9\times10^{-5}\ (\frac{M_{R_2}}{\text{TeV}})^2$
$K^0_L \to \pi^0 e^\pm\mu^\mp$	$\lvert\hat{f}^R_{d\mu}\hat{f}^{R*}_{se}-f^R_{s\mu}f^{R*}_{de}\rvert \le 2.9\times10^{-4}\ (\frac{M_{R_2}}{\text{TeV}})^2$
$K^+ \to \pi^+e^+e^-$	$\lvert\hat{f}^R_{de}\hat{f}^{R*}_{s\mu}\rvert \le 2.3\times10^{-2}\ (\frac{M_{R_2}}{\text{TeV}})^2$
$K^+ \to \pi^+e^-\mu^+$	$\lvert\hat{f}^R_{d\mu}\hat{f}^{R*}_{se}\rvert, \lvert\hat{f}^R_{de}\hat{f}^{R*}_{s\mu}\rvert \le 1.9\times10^{-4}\ (\frac{M_{R_2}}{\text{TeV}})^2$
$K-\bar{K}$	$\lvert\hat{f}^{R*}_{da}\hat{f}^R_{s\alpha}\rvert \le 0.0266\ (\frac{M_{R_2}}{\text{TeV}})$
$K^+ \to \pi^+\nu\nu$	$\text{Re}[\hat{y}^L_{de}\hat{y}^L_{se}] = [-3.7, 8.3]\times10^{-4}\ (\frac{M_{S_1}}{\text{TeV}})^2$
	$[\sum_{m\neq n}\lvert\hat{y}^L_{dm}\hat{y}^{L*}_{sn}\rvert^2]^{1/2} < 6.0\times10^{-4}\ (\frac{M_{S_1}}{\text{TeV}})^2$
$B \to K^{(*)}\nu\nu$	$\hat{y}^L_{b\alpha}\hat{y}^L_{s\beta} = [-0.036, 0.076]\ (\frac{M_{S_1}}{\text{TeV}})^2,\ [R^{\nu\bar{\nu}}_{K^*} < 2.7]$
	$\hat{y}^L_{b\alpha}\hat{y}^L_{s\beta} = [-0.047, 0.087]\ (\frac{M_{S_1}}{\text{TeV}})^2,\ [R^{\nu\bar{\nu}}_{K} < 3.9]$

Similarly, R_2 LQ in the up-quark diagonal basis leads to various kaon decay processes [203–205] for which numerous stringent bounds are listed in Table II. Moreover, the model requires $f^R_{b\tau} \sim \mathcal{O}(1)$, which modifies Z-boson decay to fermion pairs through one-loop radiative corrections. Then the LEP data [206] on the effective coupling leads to $|f^R_{b\tau}| \le 1.21$ [207] for LQ mass of 1.0 TeV.

A. Nonstandard neutrino interactions

Both R_2 and S_1 LQs have couplings to neutrinos and quarks that can induce charged-current nonstandard neutrino interactions (NSI) at tree-level [208–210]. Using the effective dimension-6 operators for NSI introduced in Ref. [208], the effective NSI parameters in our model are given by

$$\varepsilon_{\alpha\beta} = \frac{3}{4\sqrt{2}G_F}\left(\frac{f^{L\star}_{u\alpha}f^L_{u\beta}}{M^2_{R^{2/3}}} + \frac{\hat{y}^L_{d\alpha}\hat{y}^L_{d\beta}}{M^2_{S^{1/3}}}\right). \tag{6}$$

The Yukawa coupling $\hat{y}^L_{d\alpha}$ is subject to strong constraint from $K^+ \to \pi^+\nu\nu$ as shown in Table II. The couplings $f^L_{u\alpha}$ ($\alpha = e$, μ) are constrained by the nonresonant dilepton searches at LHC and the limit on f^L_{ue} and $f^L_{u\mu}$ are 0.19 and 0.16 for 1 TeV LQ mass. Thus, the contribution of $\hat{y}^L_{d\alpha}$ and $f^L_{u\alpha}$ which leads to $\varepsilon_{\alpha\beta}$ is at subpercent level. However, the LHC limits on the LQ Yukawa coupling in the tau sector are weaker and in principle be $\mathcal{O}(1)$ leading to $\epsilon_{\tau\tau}$ as large as 34.4% [210], which is within reach of long-baseline neutrino experiments, such as DUNE [211].

IV. CONSTRAINTS FROM DIRECT SEARCHES

At the LHC, S_1 and R_2 LQs can be pair produced [212–214] through gg and $q\bar{q}$ fusion processes or can be singly produced in association with charged leptons via s- and t- channel quark-gluon fusion processes. The single production of LQ becomes only relevant for larger Yukawa couplings to the first and second-generation quarks [215]. Thus, collider bounds from single-production are not so significant compared to QCD-driven LQ pair production for our analysis. In both ATLAS and CMS, there are dedicated searches for the LQ pair production in different modes, $\text{LQ}^\dagger\ \text{LQ} \to q\bar{q}\ell\bar{\ell}, q\bar{q}\nu\bar{\nu}$. The collider limits on LQ mass depend on the branching ratios to different modes, as depicted in Fig. 2 (upper plot). Apart from the LQ-pair production bound, there are bounds on the couplings and mass on the LQ from the high-p_T tails of $pp \to \ell\ell$ distributions [133,140,169,174,216–220]. The corresponding bounds are also shown in Fig. 2 (lower plot).

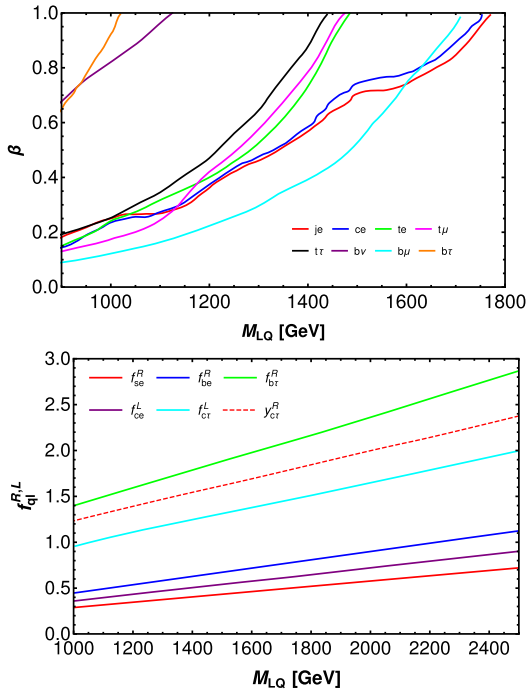

FIG. 2. Upper plot: Summary of the current limits from searches for LQ pair-production at the LHC for different quark-lepton final states. The branching ratio β varies from 0 to 1 for a specific decay channel of the LQ, while the other decay channels that are not specified compensate for the missing branching ratios. Lower plot: Upper limits on the LQ couplings $f^{R,L}$ as a function of the LQ R_2 mass are presented, obtained from recent nonresonant dilepton searches at the LHC. The red dashed line represents bound on $y^R_{c\tau}$ for S_1 LQ.

The above direct searches assume that the LQs decay promptly, which is no longer applicable for long-lived states. The colored particles arising from the ξ field can generally be long-lived if their mixing with the LQs is sufficiently small, typically required to correctly incorporate the neutrino mass scale. Colored long-lived particles (CLLPs) hadronize prior to decay, forming so-called R-hadrons [221] that are bound states composed of the CLLP and light quarks, antiquarks, and gluons. Since these particles

carry color charge, for TeV scale masses, they are efficiently pair-produced $pp \to \chi_a \bar{\chi}_a$ via pure QCD interactions. Once produced, they decay to SM fermions with decay width $\Gamma \sim y^2 m_\chi/(16\pi)$ [222] corresponding to a vertex displacement of $d \sim 10^{-14}/y^2$ mm. Therefore, for Yukawa couplings $y \gtrsim 10^{-6.5}$, decay is prompt since the corresponding vertex displacements are smaller than typical LHC detector resolution [212]. On the other hand, for $y \lesssim 10^{-6.5}$ they become long-lived, and for $y \lesssim 10^{-9}$ these states are practically stable and decay outside the detector. Long-lived gluinos and squarks have been extensively searched for at the LHC. However, no signal above the expected background is found, which provides lower bounds on the CLLPs. Our scenario is similar to the long-lived sbottom ($Q_{em} = 1/3$) and stop ($Q_{em} = 2/3$) for which the current bounds at 95% confidence level are $m \geq 1250$ GeV [223] and $m \geq 1800$ GeV [224], respectively.

V. RESULTS AND DISCUSSION

In this section, we present our numerical results and study the correlations among $R_{D^{(*)}}$, $R_{K^{(*)}}$, Δa_μ, and Δa_e anomalies within their 1σ measured values while consistently incorporating neutrino oscillations data. First, we demonstrate the viability of our proposed model by providing two benchmark points[4] given in Eqs. (7) and (11) for two distinct textures.

A. TX-I

With $m_0 I_0 = 1.73 \times 10^{-6}$ GeV, $M_{R_2} = 1.5$ TeV, and $M_{S_1} = 1.2$ TeV:

$$f^R = \begin{pmatrix} 0 & 0 & 0 \\ \mathbf{0.13} & 0 & -0.027 \\ \mathbf{0.036} & 0.01 & 0 \end{pmatrix},$$

$$f^L = \begin{pmatrix} 0 & 0 & \textit{1.0} \\ 0 & 0 & 6.36\times10^{-4} \\ 0 & 0 & -5.32\times10^{-6} \end{pmatrix},$$

$$y^R = \begin{pmatrix} 0 & 0 & 0 \\ -0.3^* & 0 & \boxed{1.0} \\ 0 & 0.0025^\dagger & 0 \end{pmatrix}, \quad y^L = \begin{pmatrix} 0 & 0 & 0 \\ 0.02^* & 0 & 0 \\ 0 & \boxed{1.2^\dagger} & 0 \end{pmatrix}. \tag{7}$$

This flavor structure explains $R_D - R_{D^*}$ (␣), $(g-2)_\mu$ (†), and $(g-2)_e$ (⋆) utilizing S_1 LQ, and $R_K - R_{K^*}$ (**bold**) from R_2 LQ. Nonzero elements in black are the additional entries required to explain neutrino oscillation data. The only nonzero entry that induces observable NSI is shown in *italics*.

B. TX-II

With $m_0 I_0 = 3.33 \times 10^{-6}$ GeV, $M_{R_2} = 1.0$ TeV, and $M_{S_1} = 1.5$ TeV:

$$f^R = \begin{pmatrix} 0 & 0 & 0 \\ \mathbf{-0.013}^* & 0 & 0 \\ \mathbf{-0.180} & 0 & \boxed{-0.9i} \end{pmatrix},$$

$$f^L = \begin{pmatrix} 0 & 0 & 0 \\ 0.3^* & 0 & \boxed{0.9} \\ 0 & 0 & 0 \end{pmatrix},$$

$$y^R = \begin{pmatrix} 0 & 0 & 0 \\ 0 & 0 & -1.85\times10^{-4} \\ 0 & 1.0^\dagger & 0 \end{pmatrix},$$

$$y^L = 10^{-3}\begin{pmatrix} 0 & 0 & 0 \\ -1.82 & 5.78i & 0 \\ 0 & 4.40^\dagger & 0 \end{pmatrix}. \tag{8}$$

This flavor structure, on the other hand, explains $R_D - R_{D^*}$ (␣), $R_K - R_{K^*}$ (**bold**), and $(g-2)_e$ (⋆) by making use of R_2 LQ, and $(g-2)_\mu$ (†) from S_1 LQ. For each of these textures, fitted neutrino observables are presented in Table III, which is in excellent agreement with experimental data. The consistency of these benchmarks' fits with the current LHC bounds are discussed later in this section.

Fits presented in Eqs. (7) and (11) incorporate the $(g-2)_e$ measurement of Ref. [5]. Here we clearly demonstrate how to consistently reproduce the more recent measurement of Ref. [59]. Interestingly, for fit Eq. (7), the coupling y^R_{21} does not play any role in neutrino mass generation. Hence reducing its size by a factor of $\sim 1/2$ and flipping its sign (to be precise, the new value is $y^R_{21} = 0.17$) reproduces the result of Ref. [59] without affecting any other observable. On the other hand, for fit Eq. (11) to replicate the measurement of Ref. [59], f^R_{21} needs to be reduced while keeping its product with f^R_{31} same. Moreover, the couplings $f^R_{21,31}$ play an insignificant role in neutrino mass generation as it is always accompanied by electron mass [i.e., suppressed by a factor of m_e/m_t, see Eq. (3)]. For instance, $f^R_{21} = 0.0093$ and $f^R_{31} = 0.252$ correctly reproduce the fit values illustrated in Table III as TX-II, while reproducing the $(g-2)_e$ result of Ref. [59].

It is worth noting that our model can, in fact, be simultaneously consistent with both values of $(g-2)_e$ inferred from Cs [5] and Rb [59] experiments. To illustrate this, we need to combine the two uncorrelated values $a_{e,\mathrm{Cs}} \pm \sigma_{\mathrm{Cs}}$ and $a_{e,\mathrm{Rb}} \pm \sigma_{\mathrm{Rb}}$ of the same physical quantity a_e to get the best estimate $a_e^{\mathrm{comb}} \pm \sigma^{\mathrm{comb}}$ via [228]

[4]In our numerical analysis, CKM matrix is expressed in terms of Wolfenstein parametrization [225] with $\lambda = 0.2248$, $A = 0.8235$, $\rho = 0.1569$. For the low scale up-type quark masses, we take $m_u(2\ \mathrm{GeV}) = 2.16$ MeV, $m_c(m_c) = 1.27$ GeV, and $m_t(m_t) = 160$ GeV, which are then extrapolated to the LQ mass scale at 1 TeV [226].

TABLE III. 3σ allowed ranges of the neutrino oscillation parameters are taken from a recent global fit [227]. 1σ allowed ranges of lepton $g-2$ and $C_9^{ee}=C_{10}^{ee}$ are also summarized. The last two columns contain the fit values of the observables for each texture. For $(g-2)_e$, the number in the parenthesis in the second column corresponds to the measurement of [59], and the corresponding fitted values are given in parentheses in the third and fourth columns for TX-I and TX-II, respectively.

Oscillation parameters	3σ range NuFIT5.1 [227]	Fit values	
		TX I (NH)	TX II (IH)
$\Delta m^2_{21}(10^{-5}\ \mathrm{eV}^2)$	$6.82-8.04$	7.41	7.39
$\Delta m^2_{23}(10^{-3}\ \mathrm{eV}^2)$(IH)	$2.410-2.574$	⋯	2.53
$\Delta m^2_{31}(10^{-3}\ \mathrm{eV}^2)$(NH)	$2.43-2.593$	2.53	⋯
$\sin^2\theta_{12}$	$0.269-0.343$	0.316	0.2986
$\sin^2\theta_{23}$ (IH)	$0.410-0.613$	⋯	0.534
$\sin^2\theta_{23}$ (NH)	$0.408-0.603$	0.506	⋯
$\sin^2\theta_{13}$ (IH)	$0.02055-0.02457$	⋯	0.0227
$\sin^2\theta_{13}$ (NH)	$0.02060-0.02435$	0.0218	⋯
Observable	1σ range		
$C_9^{ee}=C_{10}^{ee}$	$[-1.65,-1.13]$ [198]	-1.39	-1.57
$(g-2)_e\ (10^{-14})$	$-88\pm36(48\pm30)$	$-86(48)$	$-84(60)$
$(g-2)_\mu\ (10^{-10})$	25.1 ± 6.0	22.4	24.2

$$a_e^{\mathrm{comb}}=\frac{\sum_k \frac{a_{e,k}}{\sigma_k^2}}{\sum_k \frac{1}{\sigma_k^2}},\qquad \sigma^{\mathrm{comb}}=\frac{1}{\sqrt{\sum_k \frac{1}{\sigma_k^2}}},\tag{9}$$

where k = Cs, Rb. For the reader's convenience, here, we collect those values of a_e inferred from the measurements of the fine-structure constant: $a_{e,\mathrm{Cs}}=0.00115965218161(23)$ [5] and $a_{e,\mathrm{Rb}}=0.00115965218025 2(95)$ [59]. Using Eq. (9), we obtain $a_e^{\mathrm{comb}}=0.00115965218045(9)$. Comparing with the direct measurement, i.e., $a_e^{\mathrm{exp}}=0.00115965218073(28)$ [6], we find a deviation

$$\Delta a_e^{\mathrm{comb}}=a_e^{\mathrm{exp}}-a_e^{\mathrm{comb}}=(2.8\pm2.9)\times10^{-13},\tag{10}$$

which clearly indicates that a_e^{exp} is in a good agreement with the (combined) SM value. The error in Eq. (10) is obtained by adding the errors of a_e^{comb} and a_e^{exp} in quadrature. Note that the combined value $\Delta a_e^{\mathrm{comb}}$ leans toward Δa_e^{Rb} due to the much smaller uncertainty associated with the Rb experiment [hence a_e^{comb} is heavily weighted by a_e^{Rb} in Eq. (9)].

Now, for TX-I with NH, one can turn off Yukawa coupling y_R^{21} without changing the corresponding fit (see discussion above). This choice gives no new physics contribution to electron $(g-2)$, i.e., a special case corresponding to a pure SM-like scenario with $\Delta a_e=0$. Furthermore, the combined value given in Eq. (10) can also be trivially reproduced by setting $y_R^{21}=0.095$ without affecting any other observable.

On the other hand, for IH with texture TX-II, setting $f_{21}^L=0$ would lead to the texture with $(\mathcal{M}_\nu)_{11}=(\mathcal{M}_\nu)_{22}=0$, forbidden by the oscillation data. One can however, lower the Yukawa coupling f_{21}^R while keeping its product with f_{31}^R fixed to obtain $C_9^{ee}=C_{10}^{ee}$ within 1σ. Moreover, $f_{21}^R\gtrsim0.0067$ is required to satisfy the bound $|f_{31}^R f_{33}^{R*}|<0.32\ (M_{R_2}/\mathrm{TeV})^2$ obtained from $\tau\to e\gamma$. This choice of f_{21}^R leads to $\Delta a_e\gtrsim4.32\times10^{-13}$, consistent with combined measurement given in Eq. (10).

Next we show that a slight deviation from the TX-II opens up parameter space allowing even a smaller value of Δa_e. We demonstrate the viability by the following modified texture:

1. TX-II′

With $m_0 I_0=4.77\times10^{-3}$ GeV, $M_{R_2}=1.0$ TeV, and $M_{S_1}=1.5$ TeV:

$$f^R=\begin{pmatrix}0&0&0\\ \mathbf{0.026}&0&0\\ \mathbf{0.09}&0&\boxed{-0.9i}\end{pmatrix},\quad f^L=\begin{pmatrix}0&0&0\\ 0.014&0&\boxed{0.9}\\ 0&0&0.005\,i\end{pmatrix},$$
$$y^R=\begin{pmatrix}0&0&0\\ 0&0&0\\ 0&1.0^\dagger&-0.132\,i\end{pmatrix},$$
$$y^L=10^{-3}\begin{pmatrix}0&0&0\\ 0.02&0.04&-1.21\\ 0&4.40^\dagger&0\end{pmatrix}.\tag{11}$$

The above benchmark, which is consistent with all flavor violating constrains, reproduces the central value of the

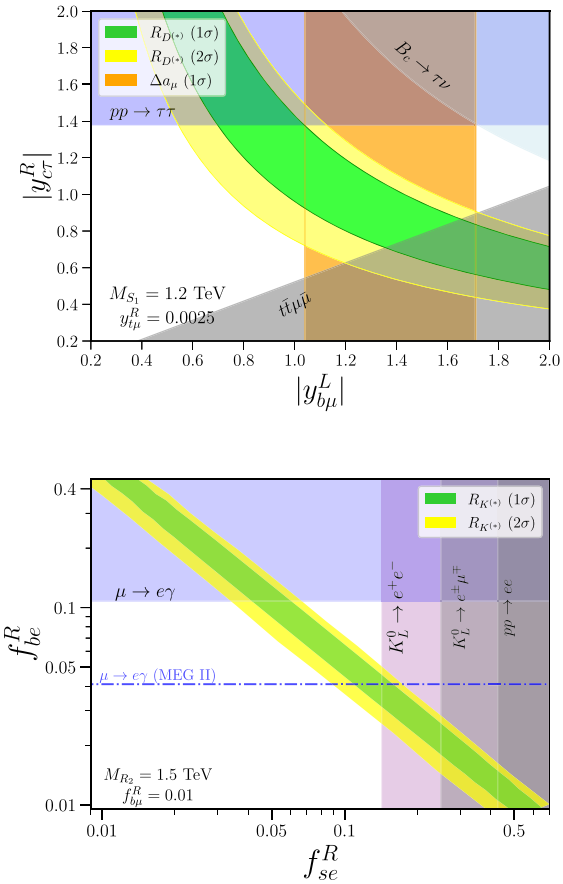

FIG. 3. TX-I: 1σ (green) and 2σ (yellow) allowed range for $R_{D^{(*)}}$ (top) and $R_{K^{(*)}}$ (bottom) in the relevant Yukawa coupling planes, with the S_1 (R_2) LQ mass fixed at 1.2 (1.5) TeV. Orange band on the top figure corresponds to 1σ allowed range of Δa_μ.

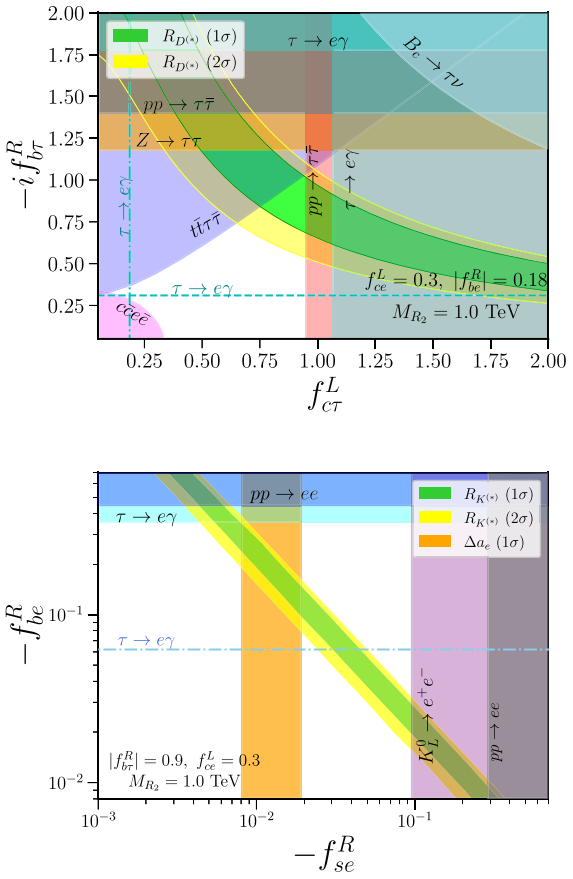

FIG. 4. TX-II: 1σ (green) and 2σ (yellow) allowed range for $R_{D^{(*)}}$ (top) and $R_{K^{(*)}}$ (bottom) in the relevant Yukawa coupling planes, with the R_2 LQ mass fixed at 1.0 TeV. Orange band on the bottom figure corresponds to 1σ allowed range of Δa_e.

neutrino observables NuFIT5.1 [227] and returns same values for the rest of the observables as in TX-II, except for $(g-2)_e$, which is found to be $\Delta a_e = 7.7 \times 10^{-14}$. This number is also fully consistent with the combined Δa_e given in Eq. (10).

Next, we study the correlations among numerous observables associated with the benchmark scenarios, TX-I and TX-II. For TX-I, the allowed parameter space to explain $R_{D^{(*)}}$ and $R_{K^{(*)}}$ at 1σ (green shaded) and 2σ (yellow shaded) CL in the relevant Yukawa coupling planes are illustrated in Fig. 3 by fixing R_2 (S_1) mass at 1.2 (1.5) TeV. In computing $R_{D^{(*)}}$ and $R_{K^{(*)}}$ observables, we utilized FLAVIO package [63]. By fixing $y^R_{t\mu} = 0.0025$ [cf. Eq. (7)], the allowed range to incorporate Δa_μ at 1σ is shown in orange band that corresponds to $y^R_{t\mu} y^L_{t\mu} \sim 10^{-3}$. We also show the exclusion regions obtained from resonant ($t\bar{t}\mu\bar{\mu}$) and nonresonant ($pp \to \tau\tau, ee$) production of LQs, along with flavor constraints such as $\mu \to e\gamma$ for a fixed $f^R_{b\mu}$, and kaon decays. Here the remaining anomaly Δa_e is determined by the product $y^R_{ce} y^L_{ce}$, and the corresponding fitted value is listed in Table III obtained from the fit Eq. (7).

Similarly, Fig. 4 illustrates the TX-II scenario where R_2 LQ addresses $R_{D^{(*)}}$, $R_{K^{(*)}}$, and Δa_e anomalies. Green and yellow bands correspond to 1σ and 2σ allowed ranges for $R_{D^{(*)}}$ and $R_{K^{(*)}}$, respectively, whereas orange band shows 1σ preferred value for Δa_e. In this plot, $M_{R_2} = 1$ TeV and $f^L_{ce} = 0.3$ [cf. Eq. (11)] are kept fixed. The exclusion regions are obtained from resonant ($t\bar{t}\tau\bar{\tau}$, $c\bar{c}e\bar{e}$) and nonresonant ($pp \to \tau\tau, ee$) production of LQs, along with flavor constraints such as $\tau \to e\gamma$ for a fixed $f^R_{b\tau}$ and f^R_{be}, kaon decays, and Z-boson decay $Z \to \tau\tau$. Δa_μ, which is not depicted in the figure, is determined by the product $y^R_{t\mu} y^L_{t\mu}$, and the corresponding benchmark value is shown in Table III obtained from Eq. (11).

As can be seen from these plots, the valid parameter space addressing all the anomalies is very limited due to various collider and flavor violating constraints, and upcoming experiments searching for LVF [200,229] have the potential to rule out this scenario. On the other hand, a resolution to flavor anomalies, particularly the $R_{D^{(*)}}$ ratios, requires LQ masses not higher than $\mathcal{O}(1)$ TeV, making this model fully testable at future high-luminosity LHC.

C. LHC bounds on fits TX-I and TX-II

For TX-I with $f^L_{u\tau} = 0$ (contributing to only NSI), R_2 LQ primarily decays to $jje\bar{e}$ and $c\bar{c}e\bar{e}$ [230] with the same Yukawa coupling f^R_{se} leading to branching ratio $\beta = 0.5$. Here we fix R_2 mass at 1.5 TeV (corresponding to branching ratio $\beta \simeq 0.74$ to $jjee$). Moreover, once $f^L_{u\tau} \sim \mathcal{O}(1)$ is included, new modes open up, and R_2 primarily decays to $jj\tau\bar{\tau}$ and $jj\nu\bar{\nu}$ [231]. There are no dedicated searches for $jj\tau\bar{\tau}$ and the limits from $jj\nu\bar{\nu}$ is 1.0 TeV for $\beta = 1$. On the other hand, for the TX-II, R_2 dominantly decays to $t\bar{t}\tau\bar{\tau}$ [232], $b\bar{b}\tau\bar{\tau}$ [233,234], $jj\tau\bar{\tau}$, and $jj\nu\nu$ each with the branching ratio $\beta \simeq 0.24$. Here we fix R_2 mass at 1 TeV, which allows the corresponding branching ratio to be as large as $\beta \simeq 0.27$ (from $t\bar{t}\tau\bar{\tau}$).

On the other hand, for TX-I, S_1 primarily decays to $jj\tau\bar{\tau}$, $t\bar{t}\mu\bar{\mu}$ [235], and $b\bar{b}\nu\bar{\nu}$ [231] with the branching ratios (0.26, 0.37, 0.37), respectively. The latter two provide limits on the scalar LQ to be 1.5 (1.2) TeV and 1.1 (0.8) TeV for branching fraction $\beta = 1(\beta = 0.5)$, which is easily satisfied for our choice of S_1 LQ mass of 1.2 TeV. Similarly, for the TX-II S_1 decays to $t\bar{t}\mu\bar{\mu}$ 100% of the time with the bound of 1.5 TeV as previously mentioned. For TX-II, we fix S_1 LQ mass at 1.5 TeV such that current collider constraints along with all the flavor constraints are easily satisfied.

The bounds from dilepton final states ($qq \to \ell\ell$) [236–238] on the relevant couplings $f^R_{se}, f^R_{be}, f^R_{b\tau}$, and $f^L_{c\tau}$ for R_2 LQ, respectively, read as (0.29,0.44,1.4,1.0) for 1 TeV mass and (0.43,0.67,1.88,1.31) for 1.5 TeV mass. Similarly, for S_1 LQ the relevant Yukawa coupling $y^R_{c\tau}$ is constrained to be 1.39 (1.61) for 1.2 (1.5) TeV mass.

Finally, we discuss the collider bounds on the states mostly originating from ξ. For our fits, using the definition of m_0 ($\sim 6 \times 10^{-3}$ GeV), we find $I_0 \sim 2 \times 10^{-4}$. Moreover, for all physical scalars with masses close to each other (i.e., $r_{ba} \ll 1$), utilizing Eqs. (4) and (5), we obtain $I_0 \approx 2 \sin 2\theta \sin 2\phi$. Then, assuming mixings of similar order, we obtain $\theta \sim \phi \sim 10^{-2}$. Therefore, states arising primarily from ξ have Yukawa couplings of order 10^{-2} with the third generation fermions (couplings with the first and second generations are more suppressed), hence decay promptly. Consequently, collider bounds on these states are identical to the bounds on LQs.

VI. CONCLUSIONS

In this Article, we have presented for the first time a two-loop radiative neutrino mass model consisting of two scalars LQs $S_1(\bar{3}, 1, 1/3)$ and $R_2(3, 2, 7/6)$ and another BSM scalar $\xi(3, 3, 2/3)$ with close-knit connections with $R_{K^{(*)}}$, $R_{D^{(*)}}$, and $(g-2)_{\mu,e}$. We have performed a detailed analysis, including all relevant flavor violating and collider constraints, and presented benchmark fits showing complete consistency with anomalies and neutrino oscillation data. Furthermore, resolving these tantalizing flavor anomalies requires LQs to have masses around the TeV scale, enabling us to test this theory at the ongoing and future colliders. Finally, it is worth mentioning that the model sets several exciting avenues for future work; the implications on electric dipole moments and their correlations with the CP-violating phases in the neutrino sector, detailed analysis on LVF decays, and a dedicated collider study.

ACKNOWLEDGMENTS

The work of J. J. was supported in part by the National Research and Innovation Agency of the Republic of Indonesia via Research Support Facility Program.

[1] G. W. Bennett *et al.* (Muon g-2 Collaboration), Final report of the Muon E821 anomalous magnetic moment measurement at BNL, Phys. Rev. D **73**, 072003 (2006).
[2] B. Abi *et al.* (Muon g-2 Collaboration), Measurement of the Positive Muon Anomalous Magnetic Moment to 0.46 ppm, Phys. Rev. Lett. **126**, 141801 (2021).
[3] T. Aoyama *et al.*, The anomalous magnetic moment of the muon in the Standard Model, Phys. Rep. **887**, 1 (2020).
[4] P. Athron, C. Balázs, D. H. Jacob, W. Kotlarski, D. Stöckinger, and H. Stöckinger-Kim, New physics explanations of a_μ in light of the FNAL muon $g-2$ measurement, J. High Energy Phys. 09 (2021) 080.
[5] R. H. Parker, C. Yu, W. Zhong, B. Estey, and H. Mueller, Measurement of the fine-structure constant as a test of the Standard Model, Science **360**, 191 (2018).
[6] D. Hanneke, S. Fogwell, and G. Gabrielse, New Measurement of the Electron Magnetic Moment and the Fine Structure Constant, Phys. Rev. Lett. **100**, 120801 (2008).
[7] G. F. Giudice, P. Paradisi, and M. Passera, Testing new physics with the electron g-2, J. High Energy Phys. 11 (2012) 113.
[8] H. Davoudiasl and W. J. Marciano, Tale of two anomalies, Phys. Rev. D **98**, 075011 (2018).
[9] A. Crivellin, M. Hoferichter, and P. Schmidt-Wellenburg, Combined explanations of $(g-2)_{\mu,e}$ and implications for a large muon EDM, Phys. Rev. D **98**, 113002 (2018).
[10] J. Liu, C. E. M. Wagner, and X.-P. Wang, A light complex scalar for the electron and muon anomalous magnetic moments, J. High Energy Phys. 03 (2019) 008.

[11] B. Dutta and Y. Mimura, Electron $g-2$ with flavor violation in MSSM, Phys. Lett. B **790**, 563 (2019).

[12] X.-F. Han, T. Li, L. Wang, and Y. Zhang, Simple interpretations of lepton anomalies in the lepton-specific inert two-Higgs-doublet model, Phys. Rev. D **99**, 095034 (2019).

[13] A. Crivellin and M. Hoferichter, Combined explanations of $(g-2)_\mu$, $(g-2)_e$ and implications for a large muon EDM, Proc. Sci. ALPS2019 (**2020**) 009 [arXiv:1905.03789].

[14] M. Endo and W. Yin, Explaining electron and muon $g-2$ anomaly in SUSY without lepton-flavor mixings, J. High Energy Phys. 08 (2019) 122.

[15] M. Abdullah, B. Dutta, S. Ghosh, and T. Li, $(g-2)_{\mu,e}$ and the ANITA anomalous events in a three-loop neutrino mass model, Phys. Rev. D **100**, 115006 (2019).

[16] M. Bauer, M. Neubert, S. Renner, M. Schnubel, and A. Thamm, Axionlike Particles, Lepton-Flavor Violation and a New Explanation of a_μ and a_e, Phys. Rev. Lett. **124**, 211803 (2020).

[17] M. Badziak and K. Sakurai, Explanation of electron and muon g—2 anomalies in the MSSM, J. High Energy Phys. 10 (2019) 024.

[18] G. Hiller, C. Hormigos-Feliu, D. F. Litim, and T. Steudtner, Anomalous magnetic moments from asymptotic safety, Phys. Rev. D **102**, 071901 (2020).

[19] A. E. Cárcamo Hernández, S. F. King, H. Lee, and S. J. Rowley, Is it possible to explain the muon and electron $g-2$ in a Z' model?, Phys. Rev. D **101**, 115016 (2020).

[20] C. Cornella, P. Paradisi, and O. Sumensari, Hunting for ALPs with lepton flavor violation, J. High Energy Phys. 01 (2020) 158.

[21] M. Endo, S. Iguro, and T. Kitahara, Probing $e\mu$ flavor-violating ALP at Belle II, J. High Energy Phys. 06 (2020) 040.

[22] A. E. Cárcamo Hernández, Y. H. Velásquez, S. Kovalenko, H. N. Long, N. A. Pérez-Julve, and V. V. Vien, Fermion masses and mixings and $g-2$ anomalies in a low scale $3-3-1$ model, Eur. Phys. J. C **81**, 191 (2021).

[23] N. Haba, Y. Shimizu, and T. Yamada, Muon and electron $g-2$ and the origin of fermion mass hierarchy, Prog. Theor. Exp. Phys. **2020**, 093B05 (2020).

[24] I. Bigaran and R. R. Volkas, Getting chirality right: Single scalar leptoquark solutions to the $(g-2)_{e,\mu}$ puzzle, Phys. Rev. D **102**, 075037 (2020).

[25] S. Jana, P. K. Vishnu, and S. Saad, Resolving electron and muon $g-2$ within the 2HDM, Phys. Rev. D **101**, 115037 (2020).

[26] L. Calibbi, M. L. López-Ibáñez, A. Melis, and O. Vives, Muon and electron $g-2$ and lepton masses in flavor models, J. High Energy Phys. 06 (2020) 087.

[27] C.-H. Chen and T. Nomura, Electron and muon $g-2$, radiative neutrino mass, and $\ell' \to \ell\gamma$ in a $U(1)_{e-\mu}$ model, Nucl. Phys. **B964**, 115314 (2021).

[28] J.-L. Yang, T.-F. Feng, and H.-B. Zhang, Electron and muon $(g-2)$ in the B-LSSM, J. Phys. G **47**, 055004 (2020).

[29] C. Hati, J. Kriewald, J. Orloff, and A. M. Teixeira, Anomalies in ^{8}Be nuclear transitions and $(g-2)_{e,\mu}$: Towards a minimal combined explanation, J. High Energy Phys. 07 (2020) 235.

[30] B. Dutta, S. Ghosh, and T. Li, Explaining $(g-2)_{\mu,e}$, the KOTO anomaly and the MiniBooNE excess in an extended Higgs model with sterile neutrinos, Phys. Rev. D **102**, 055017 (2020).

[31] F. J. Botella, F. Cornet-Gomez, and M. Nebot, Electron and muon $g-2$ anomalies in general flavour conserving two Higgs doublets models, Phys. Rev. D **102**, 035023 (2020).

[32] K.-F. Chen, C.-W. Chiang, and K. Yagyu, An explanation for the muon and electron $g-2$ anomalies and dark matter, J. High Energy Phys. 09 (2020) 119.

[33] I. Doršner, S. Fajfer, and S. Saad, $\mu \to e\gamma$ selecting scalar leptoquark solutions for the $(g-2)_{e,\mu}$ puzzles, Phys. Rev. D **102**, 075007 (2020).

[34] C. Arbeláez, R. Cepedello, R. M. Fonseca, and M. Hirsch, $(g-2)$ anomalies and neutrino mass, Phys. Rev. D **102**, 075005 (2020).

[35] S. Jana, P. K. Vishnu, W. Rodejohann, and S. Saad, Dark matter assisted lepton anomalous magnetic moments and neutrino masses, Phys. Rev. D **102**, 075003 (2020).

[36] C.-K. Chua, Data-driven study of the implications of anomalous magnetic moments and lepton flavor violating processes of e, μ and τ, Phys. Rev. D **102**, 055022 (2020).

[37] E. J. Chun and T. Mondal, Explaining $g-2$ anomalies in two Higgs doublet model with vector-like leptons, J. High Energy Phys. 11 (2020) 077.

[38] S.-P. Li, X.-Q. Li, Y.-Y. Li, Y.-D. Yang, and X. Zhang, Power-aligned 2HDM: A correlative perspective on $(g-2)_{e,\mu}$, J. High Energy Phys. 01 (2021) 034.

[39] L. Delle Rose, S. Khalil, and S. Moretti, Explaining electron and muon $g-2$ anomalies in an aligned 2-Higgs doublet model with right-handed neutrinos, Phys. Lett. B **816**, 136216 (2021).

[40] K. Kowalska and E. M. Sessolo, Minimal models for g-2 and dark matter confront asymptotic safety, Phys. Rev. D **103**, 115032 (2021).

[41] A. E. C. Hernández, S. F. King, and H. Lee, Fermion mass hierarchies from vectorlike families with an extended 2HDM and a possible explanation for the electron and muon anomalous magnetic moments, Phys. Rev. D **103**, 115024 (2021).

[42] A. Bodas, R. Coy, and S. J. D. King, Solving the electron and muon $g-2$ anomalies in Z' models, Eur. Phys. J. C **81**, 1065 (2021).

[43] J. Cao, Y. He, J. Lian, D. Zhang, and P. Zhu, Electron and muon anomalous magnetic moments in the inverse seesaw extended NMSSM, Phys. Rev. D **104**, 055009 (2021).

[44] T. Mondal and H. Okada, Inverse seesaw and $(g-2)$ anomalies in $B-L$ extended two Higgs doublet model, Nucl. Phys. **B976**, 115716 (2022).

[45] A. E. Cárcamo Hernández, C. Espinoza, J. Carlos Gómez-Izquierdo, and M. Mondragón, Fermion masses and mixings, dark matter, leptogenesis and $g-2$ muon anomaly in an extended 2HDM with inverse seesaw, arXiv:2104.02730.

[46] X.-F. Han, T. Li, H.-X. Wang, L. Wang, and Y. Zhang, Lepton-specific inert two-Higgs-doublet model confronted with the new results for muon and electron g-2 anomalies and multi-lepton searches at the LHC, Phys. Rev. D **104**, 115001 (2021).

[47] P. Escribano, J. Terol-Calvo, and A. Vicente, $(g-2)_{e,\mu}$ in an extended inverse type-III seesaw model, Phys. Rev. D **103**, 115018 (2021).

[48] A. E. Cárcamo Hernández, S. Kovalenko, M. Maniatis, and I. Schmidt, Fermion mass hierarchy and g-2 anomalies in an extended 3HDM Model, J. High Energy Phys. 10 (2021) 036.

[49] W.-F. Chang, One colorful resolution to the neutrino mass generation, three lepton flavor universality anomalies, and the Cabibbo angle anomaly, J. High Energy Phys. 09 (2021) 043.

[50] T. A. Chowdhury and S. Saad, Non-Abelian vector dark matter and lepton g-2, J. Cosmol. Astropart. Phys. 10 (2021) 014.

[51] H. Bharadwaj, S. Dutta, and A. Goyal, Leptonic $g-2$ anomaly in an extended Higgs sector with vector-like leptons, J. High Energy Phys. 11 (2021) 056.

[52] D. Borah, M. Dutta, S. Mahapatra, and N. Sahu, Lepton anomalous magnetic moment with singlet-doublet fermion dark matter in scotogenic $U(1)_{L_\mu - L_\tau}$ model, Phys. Rev. D **105**, 015029 (2022).

[53] I. Bigaran and R. R. Volkas, Reflecting on Chirality: *CP*-violating extensions of the single scalar-leptoquark solutions for the $(g-2)_{e,\mu}$ puzzles and their implications for lepton EDMs, Phys. Rev. D **105**, 015002 (2022).

[54] V. Padmanabhan Kovilakam, S. Jana, and S. Saad, Electron and muon $(g-2)$ in the 2HDM, Proc. Sci. EPS-HEP2021 (**2022**) 696.

[55] H. Li and P. Wang, Solution of lepton g-2 anomalies with nonlocal QED, arXiv:2112.02971.

[56] A. Biswas and S. Khan, $(g-2)_{e,\mu}$ and strongly interacting dark matter with collider implications, J. High Energy Phys. 07 (2022) 037.

[57] R. K. Barman, R. Dcruz, and A. Thapa, Neutrino masses and magnetic moments of electron and muon in the Zee Model, J. High Energy Phys. 03 (2022) 183.

[58] T. A. Chowdhury, M. Ehsanuzzaman, and S. Saad, Dark matter and $(g-2)_{\mu,e}$ in radiative Dirac neutrino mass models, arXiv:2203.14983.

[59] L. Morel, Z. Yao, P. Cladé, and S. Guellati-Khélifa, Determination of the fine-structure constant with an accuracy of 81 parts per trillion, Nature (London) **588**, 61 (2020).

[60] S. Descotes-Genon, L. Hofer, J. Matias, and J. Virto, Global analysis of $b \to s\ell\ell$ anomalies, J. High Energy Phys. 06 (2016) 092.

[61] C. Bobeth, G. Hiller, and G. Piranishvili, Angular distributions of $\bar{B} \to \bar{K}\ell^+\ell^-$ decays, J. High Energy Phys. 12 (2007) 040.

[62] M. Bordone, G. Isidori, and A. Pattori, On the standard model predictions for R_K and R_{K^*}, Eur. Phys. J. C **76**, 440 (2016).

[63] D. M. Straub, Flavio: A Python package for flavour and precision phenomenology in the standard model and beyond, arXiv:1810.08132.

[64] G. Isidori, S. Nabeebaccus, and R. Zwicky, QED corrections in $\bar{B} \to \bar{K}\ell^+\ell^-$ at the double-differential level, J. High Energy Phys. 12 (2020) 104.

[65] R. Aaij *et al.* (LHCb Collaboration), Test of lepton universality with $B^0 \to K^{*0}\ell^+\ell^-$ decays, J. High Energy Phys. 08 (2017) 055.

[66] R. Aaij *et al.* (LHCb Collaboration), Search for Lepton-Universality Violation in $B^+ \to K^+\ell^+\ell^-$ Decays, Phys. Rev. Lett. **122**, 191801 (2019).

[67] A. Abdesselam *et al.* (Belle Collaboration), Test of Lepton-Flavor Universality in $B \to K^*\ell^+\ell^-$ Decays at Belle, Phys. Rev. Lett. **126**, 161801 (2021).

[68] S. Choudhury *et al.* (BELLE Collaboration), Test of lepton flavor universality and search for lepton flavor violation in $B \to K\ell\ell$ decays, J. High Energy Phys. 03 (2021) 105.

[69] R. Aaij *et al.* (LHCb Collaboration), Test of lepton universality in beauty-quark decays, Nat. Phys. **18**, 277 (2022).

[70] R. Aaij *et al.* (LHCb Collaboration), Angular analysis of the $B^0 \to K^{*0}\mu^+\mu^-$ decay using 3 fb^{-1} of integrated luminosity, J. High Energy Phys. 02 (2016) 104.

[71] R. Aaij *et al.* (LHCb Collaboration), Angular analysis of the $B^0 \to K^{*0}e^+e^-$ decay in the low $-$ q^2 region, J. High Energy Phys. 04 (2015) 064.

[72] R. Aaij *et al.* (LHCb Collaboration), Measurements of the S-wave fraction in $B^0 \to K^+\pi^-\mu^+\mu^-$ decays and the $B^0 \to K^*(892)^0\mu^+\mu^-$ differential branching fraction, J. High Energy Phys. 11 (2016) 047; 04 (2017) 142(E).

[73] S. Wehle *et al.* (Belle Collaboration), Lepton-Flavor-Dependent Angular Analysis of $B \to K^*\ell^+\ell^-$, Phys. Rev. Lett. **118**, 111801 (2017).

[74] M. Aaboud *et al.* (ATLAS Collaboration), Angular analysis of $B_d^0 \to K^*\mu^+\mu^-$ decays in pp collisions at $\sqrt{s} =$ 8 TeV with the ATLAS detector, J. High Energy Phys. 10 (2018) 047.

[75] V. Khachatryan *et al.* (CMS Collaboration), Angular analysis of the decay $B^0 \to K^{*0}\mu^+\mu^-$ from pp collisions at $\sqrt{s} = 8$ TeV, Phys. Lett. B **753**, 424 (2016).

[76] A. M. Sirunyan *et al.* (CMS Collaboration), Measurement of angular parameters from the decay $\text{B}^0 \to \text{K}^{*0}\mu^+\mu^-$ in proton-proton collisions at $\sqrt{s} = 8$ TeV, Phys. Lett. B **781**, 517 (2018).

[77] R. Aaij *et al.* (LHCb Collaboration), Measurement of *CP*-Averaged Observables in the $B^0 \to K^{*0}\mu^+\mu^-$ Decay, Phys. Rev. Lett. **125**, 011802 (2020).

[78] R. Aaij *et al.* (LHCb Collaboration), Angular Analysis of the $B^+ \to K^{*+}\mu^+\mu^-$ Decay, Phys. Rev. Lett. **126**, 161802 (2021).

[79] R. Aaij *et al.* (LHCb Collaboration), Angular analysis and differential branching fraction of the decay $B_s^0 \to \phi\mu^+\mu^-$, J. High Energy Phys. 09 (2015) 179.

[80] B. Capdevila, A. Crivellin, S. Descotes-Genon, J. Matias, and J. Virto, Patterns of New Physics in $b \to s\ell^+\ell^-$ transitions in the light of recent data, J. High Energy Phys. 01 (2018) 093.

[81] J. Aebischer, W. Altmannshofer, D. Guadagnoli, M. Reboud, P. Stangl, and D. M. Straub, B-decay discrepancies after Moriond 2019, Eur. Phys. J. C **80**, 252 (2020).

[82] J. P. Lees *et al.* (*BABAR* Collaboration), Measurement of an excess of $\bar{B} \to D^{(*)}\tau^-\bar{\nu}_\tau$ decays and implications for charged Higgs bosons, Phys. Rev. D **88**, 072012 (2013).

[83] S. Hirose *et al.* (Belle Collaboration), Measurement of the τ Lepton Polarization and $R(D^*)$ in the Decay $\bar{B} \to D^* \tau^- \bar{\nu}_\tau$, Phys. Rev. Lett. **118**, 211801 (2017).

[84] R. Aaij *et al.* (LHCb Collaboration), Measurement of the Ratio of Branching Fractions $\mathcal{B}(\bar{B}^0 \to D^{*+} \tau^- \bar{\nu}_\tau)/\mathcal{B}(\bar{B}^0 \to D^{*+} \mu^- \bar{\nu}_\mu)$, Phys. Rev. Lett. **115**, 111803 (2015).

[85] R. Aaij *et al.* (LHCb Collaboration), Test of lepton flavor universality by the measurement of the $B^0 \to D^{*-} \tau^+ \nu_\tau$ branching fraction using three-prong τ decays, Phys. Rev. D **97**, 072013 (2018).

[86] A. Abdesselam *et al.* (Belle Collaboration), Measurement of $\mathcal{R}(D)$ and $\mathcal{R}(D^*)$ with a semileptonic tagging method, arXiv:1904.08794.

[87] H. Na, C. M. Bouchard, G. P. Lepage, C. Monahan, and J. Shigemitsu (HPQCD Collaboration), $B \to Dl\nu$ form factors at nonzero recoil and extraction of $|V_{cb}|$, Phys. Rev. D **92**, 054510 (2015).

[88] S. Aoki *et al.*, Review of lattice results concerning low-energy particle physics, Eur. Phys. J. C **77**, 112 (2017).

[89] Y. S. Amhis *et al.* (HFLAV Collaboration), Averages of b-hadron, c-hadron, and τ-lepton properties as of 2018, Eur. Phys. J. C **81**, 226 (2021).

[90] Y. Cai, J. Herrero-Garcia, M. A. Schmidt, A. Vicente, and R. R. Volkas, From the trees to the forest: A review of radiative neutrino mass models, Front. Phys. **5**, 63 (2017).

[91] Y. Cai, T. Han, T. Li, and R. Ruiz, Lepton number violation: Seesaw models and their collider tests, Front. Phys. **6**, 40 (2018).

[92] J. Julio, S. Saad, and A. Thapa, A tale of flavor anomalies and the origin of neutrino mass, arXiv:2202.10479.

[93] I. Doršner, S. Fajfer, A. Greljo, J. F. Kamenik, and N. Košnik, Physics of leptoquarks in precision experiments and at particle colliders, Phys. Rep. **641**, 1 (2016).

[94] M. Tanaka and R. Watanabe, New physics in the weak interaction of $\bar{B} \to D^{(*)} \tau \bar{\nu}$, Phys. Rev. D **87**, 034028 (2013).

[95] I. Doršner, S. Fajfer, N. Košnik, and I. Nišandšić, Minimally flavored colored scalar in $\bar{B} \to D^{(*)} \tau \bar{\nu}$ and the mass matrices constraints, J. High Energy Phys. 11 (2013) 084.

[96] Y. Sakaki, M. Tanaka, A. Tayduganov, and R. Watanabe, Testing leptoquark models in $\bar{B} \to D^{(*)} \tau \bar{\nu}$, Phys. Rev. D **88**, 094012 (2013).

[97] M. Duraisamy, P. Sharma, and A. Datta, Azimuthal $B \to D^* \tau^- \overline{\nu_\tau}$ angular distribution with tensor operators, Phys. Rev. D **90**, 074013 (2014).

[98] G. Hiller and M. Schmaltz, R_K and future $b \to s\ell\ell$ physics beyond the standard model opportunities, Phys. Rev. D **90**, 054014 (2014).

[99] A. J. Buras, J. Girrbach-Noe, C. Niehoff, and D. M. Straub, $B \to K^{(*)} \nu \bar{\nu}$ decays in the standard model and beyond, J. High Energy Phys. 02 (2015) 184.

[100] B. Gripaios, M. Nardecchia, and S. A. Renner, Composite leptoquarks and anomalies in B-meson decays, J. High Energy Phys. 05 (2015) 006.

[101] M. Freytsis, Z. Ligeti, and J. T. Ruderman, Flavor models for $\bar{B} \to D^{(*)} \tau \bar{\nu}$, Phys. Rev. D **92**, 054018 (2015).

[102] H. Päs and E. Schumacher, Common origin of R_K and neutrino masses, Phys. Rev. D **92**, 114025 (2015).

[103] M. Bauer and M. Neubert, Minimal Leptoquark Explanation for the $R_{D^{(*)}}$, R_K, and $(g-2)_g$ Anomalies, Phys. Rev. Lett. **116**, 141802 (2016).

[104] S. Fajfer and N. Košnik, Vector leptoquark resolution of R_K and $R_{D^{(*)}}$ puzzles, Phys. Lett. B **755**, 270 (2016).

[105] F. F. Deppisch, S. Kulkarni, H. Päs, and E. Schumacher, Leptoquark patterns unifying neutrino masses, flavor anomalies, and the diphoton excess, Phys. Rev. D **94**, 013003 (2016).

[106] X.-Q. Li, Y.-D. Yang, and X. Zhang, Revisiting the one leptoquark solution to the $R(D^{(*)})$ anomalies and its phenomenological implications, J. High Energy Phys. 08 (2016) 054.

[107] D. Bečirević, S. Fajfer, N. Košnik, and O. Sumensari, Leptoquark model to explain the B-physics anomalies, R_K and R_D, Phys. Rev. D **94**, 115021 (2016).

[108] D. Bečirević, N. Košnik, O. Sumensari, and R. Zukanovich Funchal, Palatable leptoquark scenarios for lepton flavor violation in exclusive $b \to s\ell_1\ell_2$ modes, J. High Energy Phys. 11 (2016) 035.

[109] S. Sahoo, R. Mohanta, and A. K. Giri, Explaining the R_K and $R_{D^{(*)}}$ anomalies with vector leptoquarks, Phys. Rev. D **95**, 035027 (2017).

[110] B. Bhattacharya, A. Datta, J.-P. Guévin, D. London, and R. Watanabe, Simultaneous explanation of the R_K and $R_{D^{(*)}}$ Puzzles: A model analysis, J. High Energy Phys. 01 (2017) 015.

[111] M. Duraisamy, S. Sahoo, and R. Mohanta, Rare semileptonic $B \to K(\pi) l_i^- l_j^+$ decay in a vector leptoquark model, Phys. Rev. D **95**, 035022 (2017).

[112] R. Barbieri, C. W. Murphy, and F. Senia, B-decay anomalies in a composite leptoquark model, Eur. Phys. J. C **77**, 8 (2017).

[113] A. Crivellin, D. Müller, and T. Ota, Simultaneous explanation of $R(D^{(*)})$ and $b \to s\mu^+\mu^-$: The last scalar leptoquarks standing, J. High Energy Phys. 09 (2017) 040.

[114] G. D'Amico, M. Nardecchia, P. Panci, F. Sannino, A. Strumia, R. Torre, and A. Urbano, Flavour anomalies after the R_{K^*} measurement, J. High Energy Phys. 09 (2017) 010.

[115] G. Hiller and I. Nisandzic, R_K and R_{K^*} beyond the Standard Model, Phys. Rev. D **96**, 035003 (2017).

[116] D. Bečirević and O. Sumensari, A leptoquark model to accommodate $R_K^{\rm exp} < R_K^{\rm SM}$ and $R_{K^*}^{\rm exp} < R_{K^*}^{\rm SM}$, J. High Energy Phys. 08 (2017) 104.

[117] Y. Cai, J. Gargalionis, M. A. Schmidt, and R. R. Volkas, Reconsidering the one leptoquark solution: Flavor anomalies and neutrino mass, J. High Energy Phys. 10 (2017) 047.

[118] A. K. Alok, B. Bhattacharya, A. Datta, D. Kumar, J. Kumar, and D. London, New physics in $b \to s\mu^+\mu^-$ after the measurement of R_{K^*}, Phys. Rev. D **96**, 095009 (2017).

[119] O. Sumensari, Leptoquark models for the B-physics anomalies, in *Proceedings of the 52nd Rencontres de Moriond on Electroweak Interactions and Unified Theories: La Thuile, Italy, 2017* (2017), pp. 445–448, arXiv:1705.07591.

[120] D. Buttazzo, A. Greljo, G. Isidori, and D. Marzocca, B-physics anomalies: A guide to combined explanations, J. High Energy Phys. 11 (2017) 044.

[121] A. Crivellin, D. Müller, A. Signer, and Y. Ulrich, Correlating lepton flavor universality violation in B decays with $\mu \to e\gamma$ using leptoquarks, Phys. Rev. D **97**, 015019 (2018).

[122] S.-Y. Guo, Z.-L. Han, B. Li, Y. Liao, and X.-D. Ma, Interpreting the $R_{K^{(*)}}$ anomaly in the colored Zee–Babu model, Nucl. Phys. **B928**, 435 (2018).

[123] D. Aloni, A. Dery, C. Frugiuele, and Y. Nir, Testing minimal flavor violation in leptoquark models of the $R_{K^{(*)}}$ anomaly, J. High Energy Phys. 11 (2017) 109.

[124] N. Assad, B. Fornal, and B. Grinstein, Baryon number and lepton universality violation in leptoquark and diquark models, Phys. Lett. B **777**, 324 (2018).

[125] L. Di Luzio, A. Greljo, and M. Nardecchia, Gauge leptoquark as the origin of B-physics anomalies, Phys. Rev. D **96**, 115011 (2017).

[126] L. Calibbi, A. Crivellin, and T. Li, Model of vector leptoquarks in view of the B-physics anomalies, Phys. Rev. D **98**, 115002 (2018).

[127] B. Chauhan and B. Kindra, Invoking chiral vector leptoquark to explain LFU violation in B decays, arXiv:1709.09989.

[128] J. M. Cline, B decay anomalies and dark matter from vectorlike confinement, Phys. Rev. D **97**, 015013 (2018).

[129] O. Sumensari, Lepton flavor (universality) violation in B-meson decays, Proc. Sci. EPS-HEP2017 (**2017**) 245 [arXiv:1710.08778].

[130] A. Biswas, D. K. Ghosh, S. K. Patra, and A. Shaw, $b \to c\ell\nu$ anomalies in light of extended scalar sectors, Int. J. Mod. Phys. A **34**, 1950112 (2019).

[131] D. Müller, Leptoquarks in flavour physics, EPJ Web Conf. **179**, 01015 (2018).

[132] M. Blanke and A. Crivellin, B Meson Anomalies in a Pati-Salam Model within the Randall-Sundrum Background, Phys. Rev. Lett. **121**, 011801 (2018).

[133] M. Schmaltz and Y.-M. Zhong, The leptoquark Hunter's guide: Large coupling, J. High Energy Phys. 01 (2019) 132.

[134] A. Azatov, D. Bardhan, D. Ghosh, F. Sgarlata, and E. Venturini, Anatomy of $b \to c\tau\nu$ anomalies, J. High Energy Phys. 11 (2018) 187.

[135] J.-H. Sheng, R.-M. Wang, and Y.-D. Yang, Scalar leptoquark effects in the lepton flavor violating exclusive $b \to s\ell_i^-\ell_j^+$ decays, Int. J. Theor. Phys. **58**, 480 (2019).

[136] D. Bečirević, I. Doršner, S. Fajfer, N. Košnik, D. A. Faroughy, and O. Sumensari, Scalar leptoquarks from grand unified theories to accommodate the B-physics anomalies, Phys. Rev. D **98**, 055003 (2018).

[137] C. Hati, G. Kumar, J. Orloff, and A. M. Teixeira, Reconciling B-meson decay anomalies with neutrino masses, dark matter and constraints from flavour violation, J. High Energy Phys. 11 (2018) 011.

[138] A. Azatov, D. Barducci, D. Ghosh, D. Marzocca, and L. Ubaldi, Combined explanations of B-physics anomalies: The sterile neutrino solution, J. High Energy Phys. 10 (2018) 092.

[139] Z.-R. Huang, Y. Li, C.-D. Lu, M. A. Paracha, and C. Wang, Footprints of new physics in $b \to c\tau\nu$ transitions, Phys. Rev. D **98**, 095018 (2018).

[140] A. Angelescu, D. Bečirević, D. A. Faroughy, and O. Sumensari, Closing the window on single leptoquark solutions to the B-physics anomalies, J. High Energy Phys. 10 (2018) 183.

[141] L. Da Rold and F. Lamagna, Composite Higgs and leptoquarks from a simple group, J. High Energy Phys. 03 (2019) 135.

[142] S. Balaji, R. Foot, and M. A. Schmidt, Chiral SU(4) explanation of the $b \to s$ anomalies, Phys. Rev. D **99**, 015029 (2019).

[143] S. Bansal, R. M. Capdevilla, and C. Kolda, Constraining the minimal flavor violating leptoquark explanation of the $R_{D^{(*)}}$ anomaly, Phys. Rev. D **99**, 035047 (2019).

[144] T. Mandal, S. Mitra, and S. Raz, $R_{D^{(*)}}$ motivated $\mathcal{S}_1$ leptoquark scenarios: Impact of interference on the exclusion limits from LHC data, Phys. Rev. D **99**, 055028 (2019).

[145] S. Iguro, T. Kitahara, Y. Omura, R. Watanabe, and K. Yamamoto, D* polarization vs. $R_{D^{(*)}}$ anomalies in the leptoquark models, J. High Energy Phys. 02 (2019) 194.

[146] B. Fornal, S. A. Gadam, and B. Grinstein, Left-right SU(4) vector leptoquark model for flavor anomalies, Phys. Rev. D **99**, 055025 (2019).

[147] T. J. Kim, P. Ko, J. Li, J. Park, and P. Wu, Correlation between $R_{D^{(*)}}$ and top quark FCNC decays in leptoquark models, J. High Energy Phys. 07 (2019) 025.

[148] I. de Medeiros Varzielas and J. Talbert, Simplified models of flavourful leptoquarks, Eur. Phys. J. C **79**, 536 (2019).

[149] J. Zhang, Y. Zhang, Q. Zeng, and R. Sun, New physics effects of the vector leptoquark on $\bar{B}^* \to P\tau\bar{\nu}_\tau$ decays, Eur. Phys. J. C **79**, 164 (2019); **79**, 423(E) (2019).

[150] U. Aydemir, T. Mandal, and S. Mitra, Addressing the $\mathbf{R_{D^{(*)}}}$ anomalies with an $\mathbf{S_1}$ leptoquark from $\mathbf{SO(10)}$ grand unification, Phys. Rev. D **101**, 015011 (2020).

[151] I. De Medeiros Varzielas and S. F. King, Origin of Yukawa couplings for Higgs bosons and leptoquarks, Phys. Rev. D **99**, 095029 (2019).

[152] C. Cornella, J. Fuentes-Martin, and G. Isidori, Revisiting the vector leptoquark explanation of the B-physics anomalies, J. High Energy Phys. 07 (2019) 168.

[153] A. Datta, D. Sachdeva, and J. Waite, Unified explanation of $b \to s\mu^+\mu^-$ anomalies, neutrino masses, and $B \to \pi K$ puzzle, Phys. Rev. D **100**, 055015 (2019).

[154] O. Popov, M. A. Schmidt, and G. White, R_2 as a single leptoquark solution to $R_{D^{(*)}}$ and $R_{K^{(*)}}$, Phys. Rev. D **100**, 035028 (2019).

[155] I. Bigaran, J. Gargalionis, and R. R. Volkas, A near-minimal leptoquark model for reconciling flavour anomalies and generating radiative neutrino masses, J. High Energy Phys. 10 (2019) 106.

[156] C. Hati, J. Kriewald, J. Orloff, and A. M. Teixeira, A nonunitary interpretation for a single vector leptoquark combined explanation to the B-decay anomalies, J. High Energy Phys. 12 (2019) 006.

[157] R. Coy, M. Frigerio, F. Mescia, and O. Sumensari, New physics in $b \to s\ell\ell$ transitions at one loop, Eur. Phys. J. C **80**, 52 (2020).

[158] S. Balaji and M. A. Schmidt, Unified SU(4) theory for the $R_{D^{(*)}}$ and $R_{K^{(*)}}$ anomalies, Phys. Rev. D **101**, 015026 (2020).

[159] A. Crivellin, D. Müller, and F. Saturnino, Flavor phenomenology of the leptoquark singlet-triplet model, J. High Energy Phys. 06 (2020) 020.

[160] O. Catà and T. Mannel, Linking lepton number violation with B anomalies, arXiv:1903.01799.

[161] W. Altmannshofer, P. S. B. Dev, A. Soni, and Y. Sui, Addressing $R_{D^{(*)}}$, $R_{K^{(*)}}$, muon $g-2$ and ANITA anomalies in a minimal R-parity violating supersymmetric framework, Phys. Rev. D **102**, 015031 (2020).

[162] K. Cheung, Z.-R. Huang, H.-D. Li, C.-D. Lü, Y.-N. Mao, and R.-Y. Tang, Revisit to the $b \to c\tau\nu$ transition: In and beyond the SM, Nucl. Phys. **B965**, 115354 (2021).

[163] S. Saad and A. Thapa, A common origin of neutrino masses and $R_{D^{(*)}}$, $R_{K^{(*)}}$ anomalies, Phys. Rev. D **102**, 015014 (2020).

[164] S. Saad, Combined explanations of $(g-2)_\mu$, $R_{D^{(*)}}$, $R_{K^{(*)}}$ anomalies in a two-loop radiative neutrino mass model, Phys. Rev. D **102**, 015019 (2020).

[165] P. B. Dev, R. Mohanta, S. Patra, and S. Sahoo, Unified explanation of flavor anomalies, radiative neutrino mass and ANITA anomalous events in a vector leptoquark model, Phys. Rev. D **102**, 095012 (2020).

[166] A. Crivellin, D. Müller, and F. Saturnino, Leptoquarks in oblique corrections and Higgs signal strength: Status and prospects, J. High Energy Phys. 11 (2020) 094.

[167] A. Crivellin, D. Mueller, and F. Saturnino, Correlating $h \to \mu^+\mu^-$ to the Anomalous Magnetic Moment of the Muon via Leptoquarks, Phys. Rev. Lett. **127**, 021801 (2021).

[168] V. Gherardi, D. Marzocca, and E. Venturini, Low-energy phenomenology of scalar leptoquarks at one-loop accuracy, J. High Energy Phys. 01 (2021) 138.

[169] K. S. Babu, P. S. B. Dev, S. Jana, and A. Thapa, Unified framework for B-anomalies, muon $g-2$ and neutrino masses, J. High Energy Phys. 03 (2021) 179.

[170] M. Bordone, O. Catà, T. Feldmann, and R. Mandal, Constraining flavour patterns of scalar leptoquarks in the effective field theory, J. High Energy Phys. 03 (2021) 122.

[171] A. Crivellin, C. Greub, D. Müller, and F. Saturnino, Scalar leptoquarks in leptonic processes, J. High Energy Phys. 02 (2021) 182.

[172] A. Crivellin, C. A. Manzari, M. Alguero, and J. Matias, Combined Explanation of the $Z \to \mathrm{bb}^-$ Forward-Backward Asymmetry, the Cabibbo Angle Anomaly, and $\tau \to \mu\nu\nu$ and $\mathrm{b} \to \mathrm{s}\ell^+\ell^-$ Data, Phys. Rev. Lett. **127**, 011801 (2021).

[173] C. Hati, J. Kriewald, J. Orloff, and A. M. Teixeira, The fate of $\mathbf{V_1}$ vector leptoquarks: The impact of future flavour data, Eur. Phys. J. C **81**, 1066 (2021).

[174] A. Angelescu, D. Bečirević, D. A. Faroughy, F. Jaffredo, and O. Sumensari, Single leptoquark solutions to the B-physics anomalies, Phys. Rev. D **104**, 055017 (2021).

[175] D. Marzocca and S. Trifinopoulos, Minimal Explanation of Flavor Anomalies: B-Meson Decays, Muon Magnetic Moment, and the Cabibbo Angle, Phys. Rev. Lett. **127**, 061803 (2021).

[176] A. Crivellin, D. Müller, and L. Schnell, Combined constraints on first generation leptoquarks, Phys. Rev. D **103**, 115023 (2021).

[177] P. F. Perez, C. Murgui, and A. D. Plascencia, Leptoquarks and matter unification: Flavor anomalies and the muon g-2, Phys. Rev. D **104**, 035041 (2021).

[178] A. Crivellin and L. Schnell, Complete Lagrangian and set of Feynman rules for scalar leptoquarks, Comput. Phys. Commun. **271**, 108188 (2022).

[179] D. Zhang, Radiative neutrino masses, lepton flavor mixing and muon $g-2$ in a leptoquark model, J. High Energy Phys. 07 (2021) 069.

[180] M. Bordone, M. Rahimi, and K. K. Vos, Lepton flavour violation in rare Λ_b decays, Eur. Phys. J. C **81**, 756 (2021).

[181] A. Carvunis, A. Crivellin, D. Guadagnoli, and S. Gangal, The forward-backward asymmetry in $B \to D^*\ell\nu$: One more hint for scalar leptoquarks?, Phys. Rev. D **105**, L031701 (2022).

[182] D. Marzocca, S. Trifinopoulos, and E. Venturini, From B-meson anomalies to Kaon physics with scalar leptoquarks, Eur. Phys. J. C **82**, 320 (2022).

[183] P. S. Bhupal Dev, A. Soni, and F. Xu, Hints of natural supersymmetry in flavor anomalies?, Phys. Rev. D **106**, 015014 (2022).

[184] L. Allwicher, P. Arnan, D. Barducci, and M. Nardecchia, Perturbative unitarity constraints on generic Yukawa interactions, J. High Energy Phys. 10 (2021) 129.

[185] X. Wang, Muon$(g-2)$ and Flavor Puzzles in the $U(1)_X$-gauged leptoquark model, arXiv:2108.01279.

[186] P. Bandyopadhyay, A. Karan, and R. Mandal, Distinguishing signatures of scalar leptoquarks at hadron and muon colliders, arXiv:2108.06506.

[187] S. Qian, C. Li, Q. Li, F. Meng, J. Xiao, T. Yang, M. Lu, and Z. You, Searching for heavy leptoquarks at a muon collider, J. High Energy Phys. 12 (2021) 047.

[188] O. Fischer *et al.*, Unveiling hidden physics at the LHC, Eur. Phys. J. C **82**, 665 (2022).

[189] V. Gherardi, New physics hints from flavour, Ph.D. thesis, SISSA, Trieste, 2021.

[190] A. Crivellin, J. F. Eguren, and J. Virto, Next-to-leading-order QCD matching for $\Delta F = 2$ processes in scalar leptoquark models, J. High Energy Phys. 03 (2022) 185.

[191] D. London and J. Matias, B flavour anomalies: 2021 Theoretical status report, arXiv:2110.13270.

[192] P. Bandyopadhyay, S. Jangid, and A. Karan, Constraining scalar doublet and triplet leptoquarks with vacuum stability and perturbativity, Eur. Phys. J. C **82**, 516 (2022).

[193] T. Husek, K. Monsalvez-Pozo, and J. Portoles, Constraints on leptoquarks from lepton-flavour-violating tau-lepton processes, J. High Energy Phys. 04 (2022) 165.

[194] Y. Afik, S. Bar-Shalom, K. Pal, A. Soni, and J. Wudka, Multi-lepton probes of new physics and lepton-universality in top-quark interactions, Nucl. Phys. **B980**, 115849 (2022).

[195] J. Heeck and A. Thapa, Explaining lepton-flavor nonuniversality and self-interacting dark matter with $L_\mu - L_\tau$, Eur. Phys. J. C **82**, 480 (2022).

[196] A. Crivellin, B. Fuks, and L. Schnell, Explaining the hints for lepton flavour universality violation with three S_2 leptoquark generations, J. High Energy Phys. 06 (2022) 169.

[197] T. A. Chowdhury and S. Saad, Leptoquark-vectorlike quark model for m_W (CDF), $(g-2)_\mu$, $R_{K^{(*)}}$ anomalies and neutrino mass, arXiv:2205.03917.
[198] W. Altmannshofer and P. Stangl, New physics in rare B decays after Moriond 2021, Eur. Phys. J. C **81**, 952 (2021).
[199] L. Lavoura, General formulae for $f(1) \to f(2)\gamma$, Eur. Phys. J. C **29**, 191 (2003).
[200] A. M. Baldini *et al.* (MEG Collaboration), Search for the lepton flavour violating decay $\mu^+ \to e^+\gamma$ with the full dataset of the MEG experiment, Eur. Phys. J. C **76**, 434 (2016).
[201] B. Aubert *et al.* (*BABAR* Collaboration), Searches for Lepton Flavor Violation in the Decays $\tau^\pm \to e^\pm\gamma$ and $\tau^\pm \to \mu^\pm\gamma$, Phys. Rev. Lett. **104**, 021802 (2010).
[202] W. H. Bertl *et al.* (SINDRUM II Collaboration), A search for muon to electron conversion in muonic gold, Eur. Phys. J. C **47**, 337 (2006).
[203] R. Mandal and A. Pich, Constraints on scalar leptoquarks from lepton and kaon physics, J. High Energy Phys. 12 (2019) 089.
[204] A. Ceccucci, Rare kaon decays, Annu. Rev. Nucl. Part. Sci. **71**, 113 (2021).
[205] E. Goudzovski *et al.*, New physics searches at kaon and hyperon factories, arXiv:2201.07805.
[206] S. Schael *et al.* (ALEPH, DELPHI, L3, OPAL, SLD, LEP Electroweak Working Group, SLD Electroweak Group, SLD Heavy Flavour Group), Precision electroweak measurements on the Z resonance, Phys. Rep. **427**, 257 (2006).
[207] P. Arnan, D. Becirevic, F. Mescia, and O. Sumensari, Probing low energy scalar leptoquarks by the leptonic W and Z couplings, J. High Energy Phys. 02 (2019) 109.
[208] L. Wolfenstein, Neutrino oscillations in matter, Phys. Rev. D **17**, 2369 (1978).
[209] P. S. Bhupal Dev *et al.*, Neutrino nonstandard interactions: A status report, SciPost Phys. Proc. **2**, 001 (2019).
[210] K. S. Babu, P. S. B. Dev, S. Jana, and A. Thapa, Non-standard interactions in radiative neutrino mass models, J. High Energy Phys. 03 (2020) 006.
[211] S. S. Chatterjee, P. S. B. Dev, and P. A. N. Machado, Impact of improved energy resolution on DUNE sensitivity to neutrino nonstandard interactions, J. High Energy Phys. 08 (2021) 163.
[212] B. Diaz, M. Schmaltz, and Y.-M. Zhong, The leptoquark Hunter's guide: Pair production, J. High Energy Phys. 10 (2017) 097.
[213] I. Doršner and A. Greljo, Leptoquark toolbox for precision collider studies, J. High Energy Phys. 05 (2018) 126.
[214] I. Doršner, S. Fajfer, and A. Lejlić, Novel leptoquark pair production at LHC, J. High Energy Phys. 05 (2021) 167.
[215] L. Buonocore, U. Haisch, P. Nason, F. Tramontano, and G. Zanderighi, Lepton-Quark Collisions at the Large Hadron Collider, Phys. Rev. Lett. **125**, 231804 (2020).
[216] O. J. P. Eboli and A. V. Olinto, Composite leptoquarks in hadronic colliders, Phys. Rev. D **38**, 3461 (1988).
[217] D. A. Faroughy, A. Greljo, and J. F. Kamenik, Confronting lepton flavor universality violation in B decays with high-p_T tau lepton searches at LHC, Phys. Lett. B **764**, 126 (2017).
[218] A. Greljo and D. Marzocca, High-p_T dilepton tails and flavor physics, Eur. Phys. J. C **77**, 548 (2017).
[219] A. Alves, O. J. P. t. Eboli, G. Grilli Di Cortona, and R. R. Moreira, Indirect and monojet constraints on scalar leptoquarks, Phys. Rev. D **99**, 095005 (2019).
[220] A. Angelescu, D. A. Faroughy, and O. Sumensari, Lepton flavor violation and dilepton tails at the LHC, Eur. Phys. J. C **80**, 641 (2020).
[221] G. R. Farrar and P. Fayet, Phenomenology of the production, decay, and detection of new hadronic states associated with supersymmetry, Phys. Lett. B **76**, 575 (1978).
[222] W. Buchmuller, R. Ruckl, and D. Wyler, Leptoquarks in lepton—quark collisions, Phys. Lett. B **191**, 442 (1987); **448**, 320(E) (1999).
[223] M. Aaboud *et al.* (ATLAS Collaboration), Search for heavy charged long-lived particles in the ATLAS detector in 36.1 fb^{-1} of proton-proton collision data at $\sqrt{s} = 13$ TeV, Phys. Rev. D **99**, 092007 (2019).
[224] A. M. Sirunyan *et al.* (CMS Collaboration), Search for long-lived particles using displaced jets in proton-proton collisions at $\sqrt{s} = 13$ TeV, Phys. Rev. D **104**, 012015 (2021).
[225] L. Wolfenstein, Parametrization of the Kobayashi-Maskawa Matrix, Phys. Rev. Lett. **51**, 1945 (1983).
[226] Z.-z. Xing, H. Zhang, and S. Zhou, Updated values of running quark and lepton masses, Phys. Rev. D **77**, 113016 (2008).
[227] I. Esteban, M. C. Gonzalez-Garcia, M. Maltoni, T. Schwetz, and A. Zhou, The fate of hints: Updated global analysis of three-flavor neutrino oscillations, J. High Energy Phys. 09 (2020) 178.
[228] *Particle Physics Reference Library: Volume 2: Detectors for Particles and Radiation*, edited by C. W. Fabjan and H. Schopper (Springer Nature, Cham, 2020).
[229] T. Aushev *et al.*, Physics at super B factory, arXiv:1002.5012.
[230] G. Aad *et al.* (ATLAS Collaboration), Search for pairs of scalar leptoquarks decaying into quarks and electrons or muons in $\sqrt{s} = 13$ TeV pp collisions with the ATLAS detector, J. High Energy Phys. 10 (2020) 112.
[231] A. M. Sirunyan *et al.* (CMS Collaboration), Constraints on models of scalar and vector leptoquarks decaying to a quark and a neutrino at $\sqrt{s} = 13$ TeV, Phys. Rev. D **98**, 032005 (2018).
[232] G. Aad *et al.* (ATLAS Collaboration), Search for pair production of third-generation scalar leptoquarks decaying into a top quark and a τ-lepton in pp collisions at $\sqrt{s} = 13$ TeV with the ATLAS detector, J. High Energy Phys. 06 (2021) 179.
[233] M. Aaboud *et al.* (ATLAS Collaboration), Searches for third-generation scalar leptoquarks in $\sqrt{s} = 13$ TeV pp collisions with the ATLAS detector, J. High Energy Phys. 06 (2019) 144.
[234] G. Aad *et al.* (ATLAS Collaboration), Search for new phenomena in pp collisions in final states with tau leptons, b-jets, and missing transverse momentum with the ATLAS detector, Phys. Rev. D **104**, 112005 (2021).
[235] G. Aad *et al.* (ATLAS Collaboration), Search for pair production of scalar leptoquarks decaying into first- or second-generation leptons and top quarks in proton–proton collisions at $\sqrt{s} = 13$ TeV with the ATLAS detector, Eur. Phys. J. C **81**, 313 (2021).

[236] G. Aad *et al.* (ATLAS Collaboration), Search for Heavy Higgs Bosons Decaying into Two Tau Leptons with the ATLAS Detector Using pp Collisions at $\sqrt{s} = 13$ TeV, Phys. Rev. Lett. **125**, 051801 (2020).

[237] G. Aad *et al.* (ATLAS Collaboration), Search for new nonresonant phenomena in high-mass dilepton final states with the ATLAS detector, J. High Energy Phys. 11 (2020) 005.

[238] A. M. Sirunyan *et al.* (CMS Collaboration), Search for resonant and nonresonant new phenomena in high-mass dilepton final states at $\sqrt{s} = 13$ TeV, J. High Energy Phys. 07 (2021) 208.